

Scientific Report No. 1-75/76

**SEMIANNUAL TECHNICAL REPORT
NORSAR PHASE 3**

1 July – 31 December 1975

Prepared by
K. A. Berteussen

Kjeller, 13 February 1976

Sponsored by
Advanced Research Projects Agency
ARPA Order No. 2551



VII.10 Precise Monitoring of Seismic Velocities

The physical setup for this experiment was explained in the previous report in this series (NORSAR Scientific Report No. 5-74/75). It involves a power station as a source vibrating at frequencies around 2.778 Hz, 5 seismometers (Ch 1-4 and 6 at subarray 14C), at distances from 4.7 to 13.7 km from the source, and a 6th data channel (Ch 5) where the network power of 50 Hz is input after being divided 18 times down to 2.78 Hz and properly reduced in voltage (to ± 4.6 V).

An extensive analysis has now been completed involving about 120 hours (5 days) of data. We have Fourier-analyzed altogether 425 blocks each of 10 000 samples of 10 Hz data (16 $\frac{2}{3}$ minutes per block), giving a frequency resolution of 0.001 Hz. For each block, the reference channel (Ch. 5) was first analyzed so as to find out what frequencies to analyze, which is important because the network power frequency actually fluctuates as much as $\pm 0.3\%$ around the nominal frequency, with a correlation time of sometimes only a few seconds. This corresponds to frequencies in the range 2.771 to 2.785 Hz, where our resolution gave 15 independent estimates. For each block, we then analyzed any frequency in that range at which the reference channel had stayed for at least 7% of the time, usually giving between 3 and 6 frequencies. Having established the frequencies to analyze in this way, the initial analysis involved estimating the Fourier transform for each of the 5 seismic data channels for each of the selected frequencies. These basic Fourier Transform results were then stacked on a digital tape, ready for subsequent analysis.

The way to monitor seismic velocities from these data is through the analysis of spectral phase differences. We will here only discuss 3 of the many possible combinations, namely, between the source (Ch 5) and Ch 4 (distance 13.7 km), between the source and Ch 1 (distance 4.7 km), and between Ch 1 and Ch 2. The latter two channels are the ones closest to the

source and therefore with the best signal-to-noise ratio, they have also practically the same distance to the source and are consequently essential as a control combination.

The phase estimates in Fig. VII.10.1 are obtained by summing the power spectral estimates over all the analyzed blocks of data, after some reduction. For each of the frequencies in each of the blocks we analyzed the power in the reference channel. It has been found that the quality of the phase estimates is proportional to this power level, and consequently a threshold was determined below which the data was rejected. In this way we improved the quality of the phase estimates by rejecting about 40% of the original data; in Fig. VII.10.1 it is shown that there remains between 1 and 146 blocks for each of the frequencies.

An important by-product of the phase estimates in Fig. VII.10.1 is that they actually give, albeit with considerable uncertainty, an estimate of the group velocity, either between two seismometers or between any seismometer and the source. The slope $d\phi/d\omega$ has been estimated using a weighted least squares estimation procedure, using as weights the number of blocks for each frequency (since that number is directly proportional to the stability). Once the slope is estimated, the group velocity is simply the distance divided by the slope. The group velocity results are not really as consistent as could be the impression from Fig. VII.10.1 ($v = 3.9 \pm 0.6$ and 3.8 ± 0.4 km/s); for the combinations of channels with acceptable signal-to-noise ratios the estimates actually vary between 3.0 and 5.0 km/s. However, using the group velocities arrived at in this way, and assuming the same values for the phase velocities, it is possible to estimate the total travel time and thereby the relative size of observed phase differences. It is found in this way that a precision of $\pm 10^{-3}$ for combination 1-5 corresponds to $\pm 1.2^\circ$, and for 4-5 the value is $\pm 3.6^\circ$, corresponding to the error bars in Fig. VII.10.1.

An obvious way to further improve the stability of the phase estimates is to use, instead of the values for individual frequencies, the intercept of the regression line with the center frequency. (The error bar in Fig. VII.10.1 has been placed around that value.) That is the technique used in Fig VII.10.2, where each phase estimate is the average over 200 minutes of data. On the average, there are around 30 individual spectral estimates (12 blocks and 2.5 frequencies per block) behind each data point in Fig. VII.10.2. The figure shows that there is no significant time variation in the data, and the standard deviation for combinations 1-5 and 4-5 are 1.5° and 4.0° , respectively, which is quite close to the values given above for a precision of 10^{-3} . The fact that we get the same precision for the two combinations means that the loss in signal-to-noise ratio for the greatest distance is compensated by the increased distance (by a factor of 3). Assuming now that a precision of 10^{-3} is obtained for each of the points in Fig. VII.10.2, we should by summing all the data, obtain a precision of about $10^{-3}/\sqrt{36} \approx 2 \cdot 10^{-4}$, which refers to the intercept points in Fig. VII.10.1.

This report is only preliminary, and work continues along the following lines: 1) Predict the possible influence from tidal stress variations (the 5 days analyzed here are selected so as to cover a time period when those variations are supposed to be at a maximum), 2) Further improve (by proper data reduction) and more accurately assess (from spectral variances) the precision of the already acquired data base, 3) As a continuation of the project, consider using higher harmonics of the 2.778 Hz data, which have quite good signal-to-noise ratios, and where the phase differences due to tidal effects should be larger.

H. Bungum
T. Risbo (Copenhagen)
E. Hjortenbergt (Copenhagen)

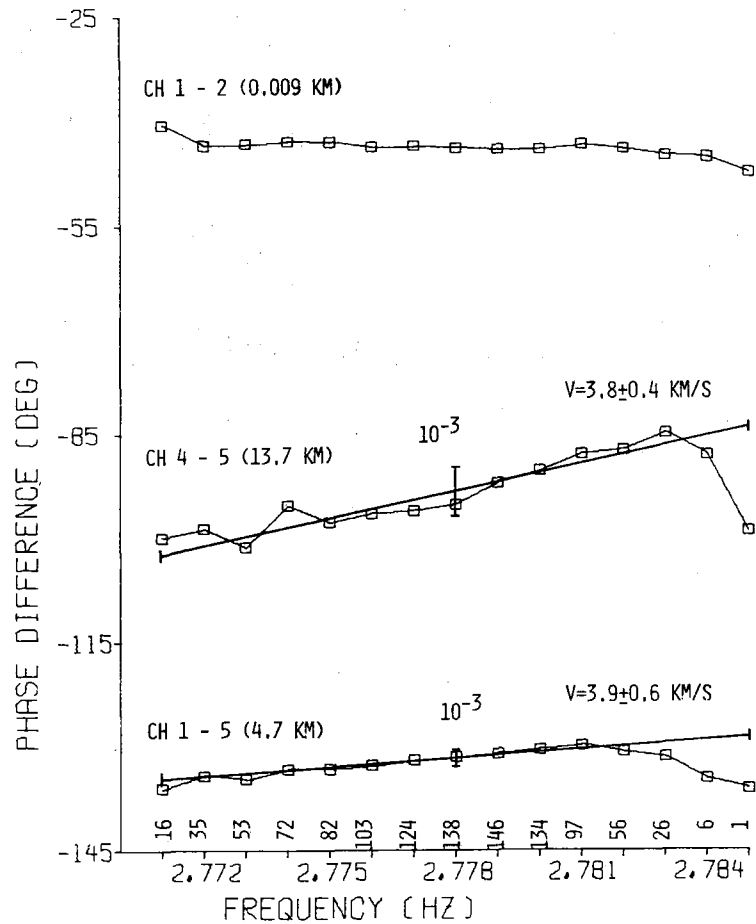


Fig. VII.10.1 Phase difference vs. frequency for three channel combinations, at sub-array 14C. The tilted numbers at the frequency axis are the number of blocks used in each estimate, which have been used as weights in a weighted least squares estimate resulting in the straight lines and the velocities given on the figure. Uncertainty bars of 10^{-3} are also given.

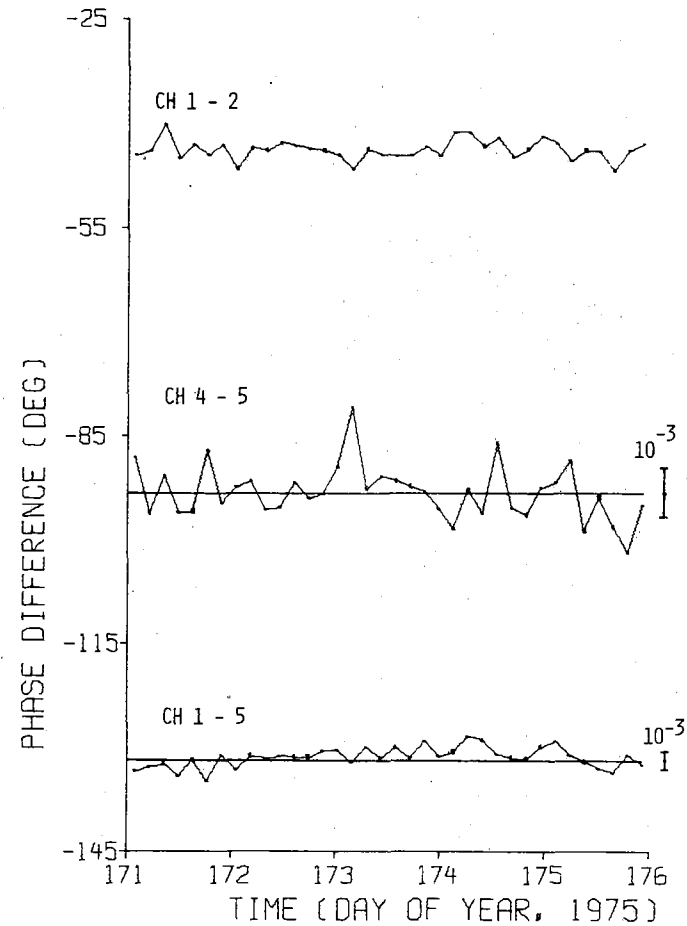


Fig. VII.10 Phase difference vs. time with 36 independent and successive estimates. The channel combinations and the uncertainty bars are the same as in Fig. VII.10.1.